Transactions on Engineering and Computing Sciences - Vol. 13, No. 06
Publication Date: November 28, 2025
DOI:10.14738/tmlai.1306.19643.
Sorescu, M., Tolea, F., & Sofronie, M. (2025). Experimental Results and Modeling of Magnetic Data for the Gallium Oxide-Hematite Mixed-Oxide Nanoparticles. *Transactions on Engineering and Computing Sciences*, 13(06). 69-78.

Experimental Results and Modeling of Magnetic Data for the Gallium Oxide-Hematite Mixed-Oxide Nanoparticles

Monica Sorescu
School of Science and Engineering,
Duquesne University, Pittsburgh, United States

Felicia Tolea
National Institute for Materials Physics,
Bucharest-Magurele, Romania

Mihaela Sofronie
National Institute for Materials Physics,
Bucharest-Magurele, Romania

ABSTRACT

The $xGa_2O_3*(1-x)a-Fe_2O_3$ (x=0.5) was prepared by mechanochemical activation using high energy ball milling for times of 0, 2, 4, 8, and 12 hours. The magnetic properties were studied by hysteresis loop measurements with an applied magnetic field of 5 T at temperatures of 5 and 300 K. Zero-field-cooling-field-cooling results were obtained in a magnetic field of 200 Oe in the temperature range 5-300 K. The magnetization and average coercive field were investigated as functions of ball milling time and temperature. They were related to changes in the average grain size, induced stresses and defects, variations in exchange coupling and magnetic ordering. ZFC did not exhibit a sharp edge, so we do not witness superparamagnetism with a well-defined blocking temperature. The Morin transition of hematite occurred over broad temperature ranges and was monitored as a function of ball milling time. The Dzyaloshinskii-Moriya antisymmetric exchange interaction explained the gradual increase in the magnetization with ball milling time.

Keywords: Hematite, Gallium Oxide, Milling, Magnetic Measurements, Coercive field.

INTRODUCTION

Hematite ($a-Fe_2O_3$) has been the focus of various theoretical and experimental studies owing to its applications as a magnetic, semiconductor and catalytic material. Doping hematite with several transition metal and rare earth elements was found to determine an improvement in its electrochemical and photocatalytic properties [1-6].

Gallium oxide (Ga_2O_3) is a paramagnetic compound that can be used to functionalize hematite with prospective applications in sensing, catalysis and flexible electronics. In particular, gallium ion Ga^{3+} was found to exhibit intriguing properties when introduced in several systems. Thus, bandgap engineering of gallium oxides by crystalline disorder emerged as a promising candidate for applications in high-power and radiofrequency electronics and deep-ultraviolet optoelectronics [7]. Defect-assisted photocatalytic activity of glass-embedded gallium oxide

nanocrystals was found to be an attractive option for the realization of smart optical fibers and self-cleaning windows [8]. Amorphous, crystallized and Mg-doped b-Ga_2O_3 thin films were investigated to understand the evolution of electronic states and related atomic arrangement [9]. Gallium oxide nanoparticles were prepared through solid state reaction route for efficient photocatalytic overall water splitting [10]. Gallium oxide nanorods were fabricated as novel, safe and durable anode materials for Li- and Na- ion batteries [11]. High-rate growth of gallium oxide films was achieved by plasma-enhanced thermal oxidation for solar-blind photodetectors [12]. Moreover, the kinetics of structural transformations during mechanical high-energy ball milling of Fe_2O_3 with Ga were investigated in order to reveal the mechanism of the process [13]. Room temperature ferromagnetism was observed in oxygen-deficient gallium oxide films with cubic spinel structure [14]. Synthesis and characterization of gallium oxide in strong reducing growth ambient were performed by chemical vapor deposition and related techniques [15]. Resistive random access memory based on gallium oxide thin films were developed for self-powered pressure sensor systems [16]. Overall, gallium oxide substitutions in hematite were found to considerably improve its technological properties and range of applications.

Recently, the ball milling technique was key to obtaining garnet-graphene nanocomposites and crucial to determine the formation of skyrmion phase in the Fe-Co-Si system. Moreover, mechanochemical activation was used to synthesize mixed-oxide nanostructures of the type $xDy_2O_3*(1-x)a-Fe_2O_3$ with the formation of solid solutions in the system [17-20].

In the present study we shed light on the magnetic properties of the $xGa_2O_3*(1-x)a-Fe_2O_3$ system with molar concentration x=0.5, obtained by mechanochemical activation at different ball milling times. Our investigations focused on hysteresis loop measurements with an applied magnetic field of 5 T at temperatures of 5 and 300 K and zero-field-cooling-field-cooling in a magnetic field of 200 Oe over the temperature range of 5-300 K.

MATERIALS AND METHODS

Nanoparticles of $xGa_2O_3*(1-x)a-Fe_2O_3$ with x=0.5 were obtained by mechanochemical activation of precursor powders of hematite and gallium oxide (Alfa Aesar) with particle sizes in the tens of nanometers range. The powders were mixed manually using a mortar and pestle and introduced in a SPEX 8000 mixer mill. They were ground for time periods ranging from 0 to 12 hours. The powder to ball mass ratio was 1:5. Magnetic property measurements were performed using a superconductor quantum interference device (SQUID) magnetometer with a 5 T magnetic field for recording hysteresis loops at 5 and 300 K and a 200 Oe magnetic field for the zero-field-cooling-field-cooling measurements in the 5-300 K temperature range. From these measurements were derived information on the magnetization and coercive fields.

RESULTS AND DISCUSSION

Magnetic measurements on the gallium oxide-hematite system at equimolar concentration were performed with an applied magnetic field of 5 T at temperatures of 5 and 300 K. Zero-field-cooling-field cooling determinations were recorded in a magnetic field of 200 Oe over the temperature range 5-300 K.

The hysteresis loops at 5 K and 300 K as well as the ZFC-FC experimental data are plotted in Figure 1 (a)-(c), respectively for the sample milled at 0 h. For the system milled for 2 h the hysteresis loops and ZFC-FC curves are displayed in Figure 2 (a)-(c), respectively. The sample milled for 4 h has the hysteresis loops and ZFC-FC determinations displayed in Figure 3 (a)-(c), respectively. For the system milled for 8 h, the hysteresis loops at 5 and 300 K and the ZFC-FC measurements are presented in Figure 4 (a)-(c), respectively. The sample milled for 12 h has the hysteresis loops and ZFC-FC data shown in Figure 5 (a)-(c), respectively.

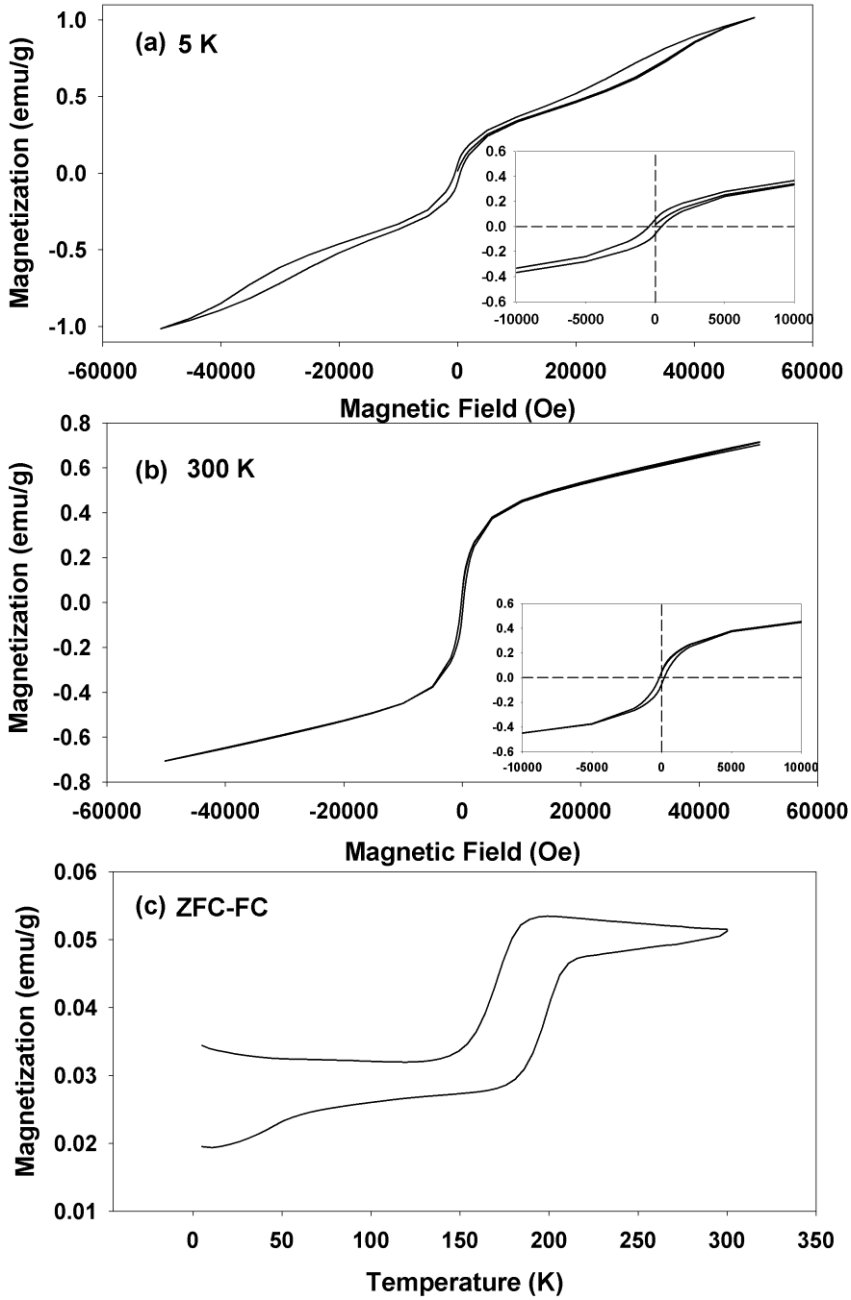

Figure 1: Hysteresis loops at 5 K (a), 300 K (b) at 5 T and ZFC-FC (c) at 200 Oe for the 0-h milled gallium oxide-hematite system.

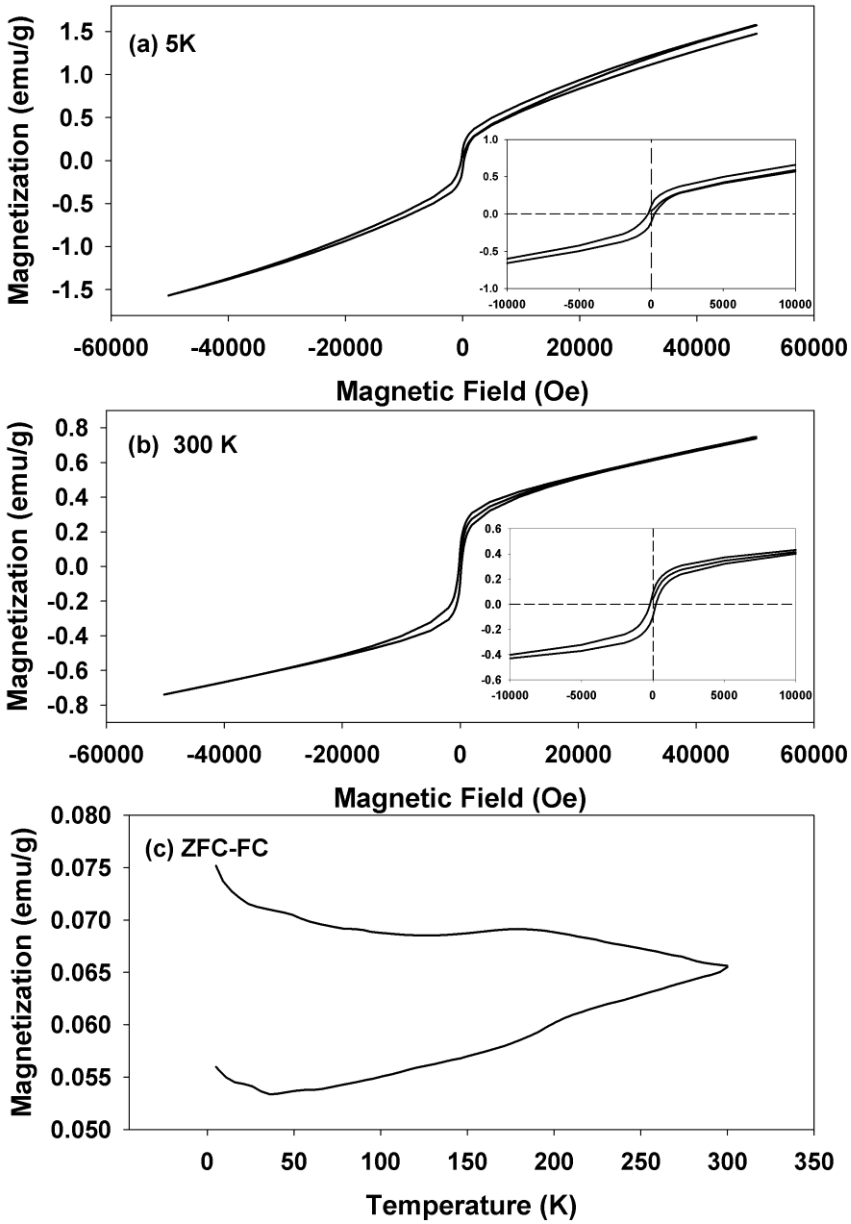

Figure 2: Hysteresis loops at 5 K (a), 300 K (b) at 5 T and ZFC-FC (c) at 200 Oe for the 2-h milled gallium oxide-hematite system.

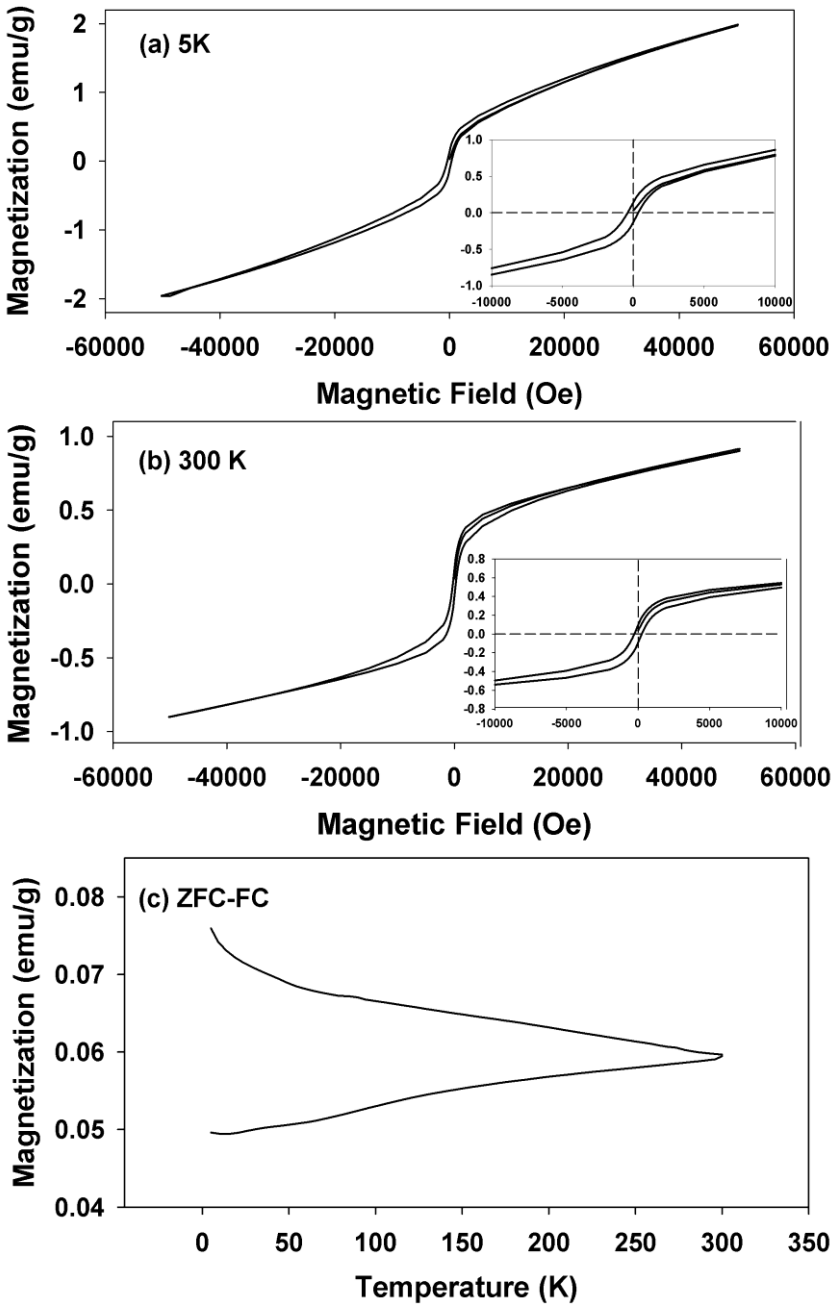

Figure 3: Hysteresis loops at 5 K (a), 300 K (b) at 5 T and ZFC-FC (c) at 200 Oe for the 4-h milled gallium oxide-hematite system.

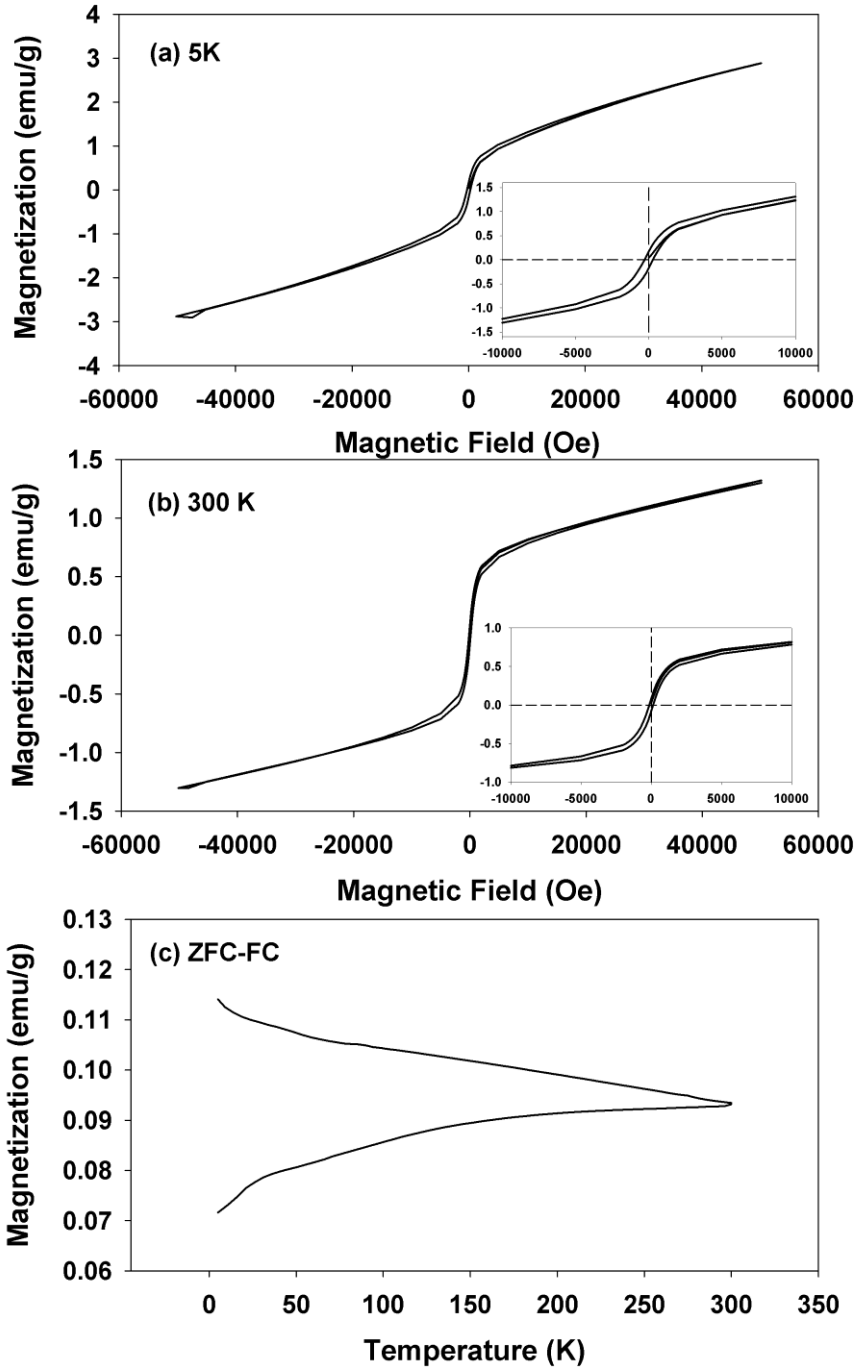

Figure 4: Hysteresis loops at 5 K (a), 300 K (b) at 5 T and ZFC-FC (c) at 200 Oe for the 8-h milled gallium oxide-hematite system.

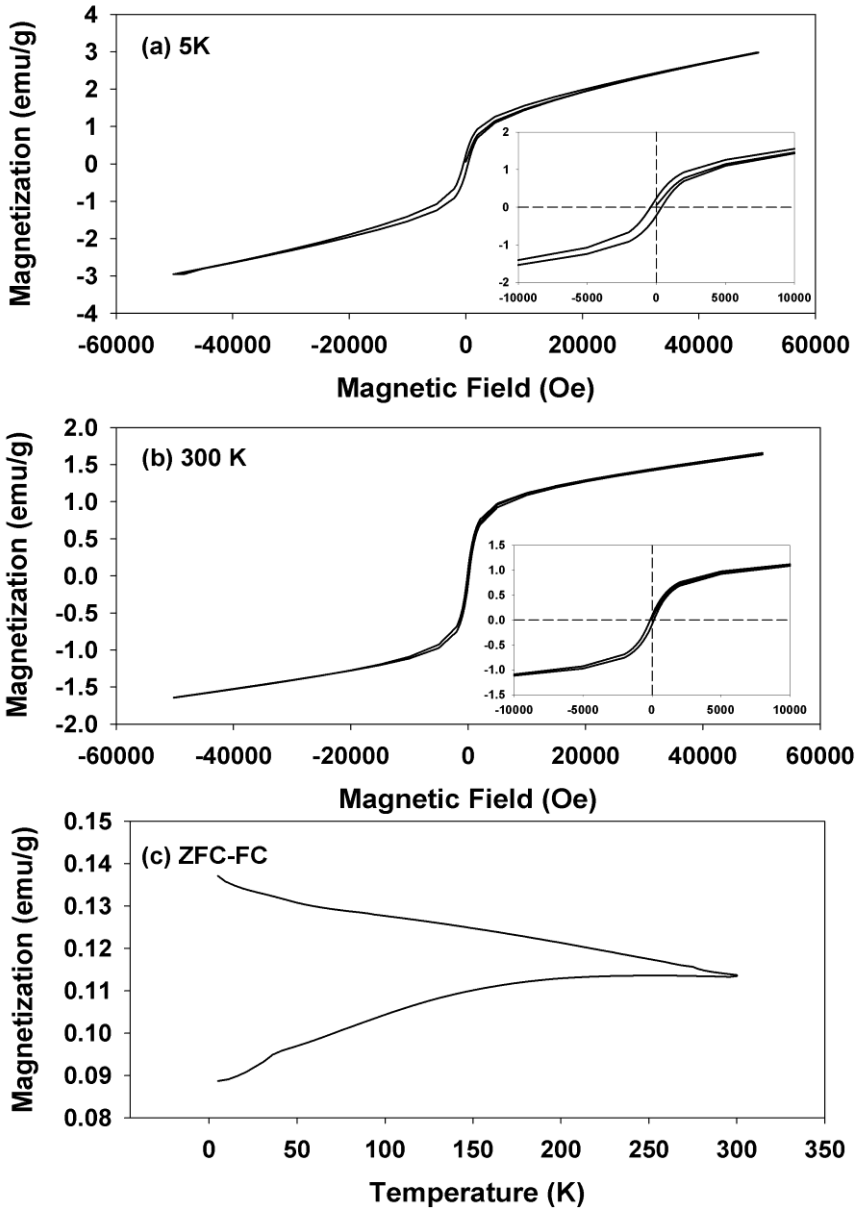

Figure 5: Hysteresis loops at 5 K (a), 300 K (b) at 5 T and ZFC-FC (c) at 200 Oe for the 12-h milled gallium oxide-hematite system.

Magnetic results indicate that there are no major structural modifications as effect of milling. The system remains described by Ga_2O_3+a-Fe_2O_3 and Ga:a-Fe_2O_3 (gallium doped hematite), with possible minute quantities of a-Fe progressively generated. The main effect is the increase in magnetization observable with the increase in the ball milling time in the ZFC-FC curves as well as in the hysteresis loops at 5 K and 300 K. The hysteresis curves show that the magnetization does not saturate for neither sample at 5 K or 300 K. The coercive field (whose values were calculated as the average between H_{c+} and H_{c-}) at 5 K does not behave monotonically neither at 5 K, nor at 300 K (Figure 6). This non-monotonical variation of the

coercive field with the milling time indicates that the milling effects are not dominated by a single mechanism (decrease in particle size), but we witness a competition between several opposing factors: increase in structural disorder, increase in microstresses, and changes in the exchange coupling which imposes magnetic ordering.

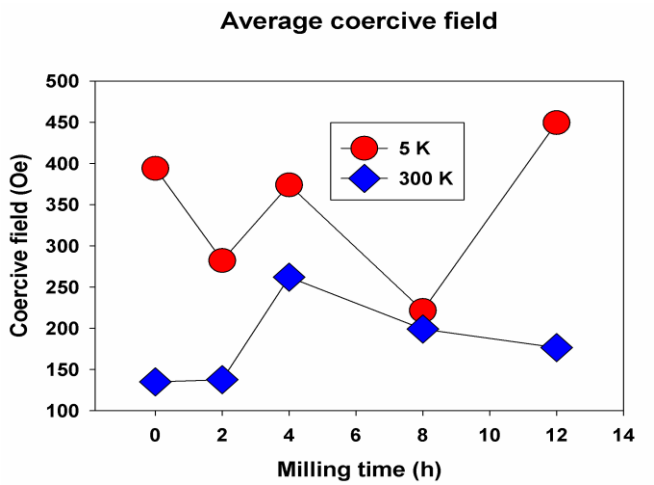

Figure 6: Average coercive field as a function of ball milling time at 5 K and 300 K.

In the beginning, (0h, 2 h) the milling process suppresses the initial ordering, such that H_c decreases (less energy stored in the initial ordered structure). After 4 h, new microstructures occur and new smaller magnetic domains (H_c increases because there is more pinning). The maximum value of H_c after 4 h of milling time at both 5 and 300 K indicates a maximum efficiency of the disorder. At longer milling times (8 and 12 h) the disorder becomes excessive and H_c becomes to decrease. The random anisotropy model [21, 22] explains very well the lack of monotonicity of the coercive field with the milling time. Initially, the decrease in the average particle size and increase in disorder lead to an increase in the collective pinning and the H_c. At long milling times, local anisotropies become independent and are statistically averaged, which determines a decrease in the coercive field.

Hematite is antiferromagnetic below the Morin temperature and becomes weak ferromagnetic above T_M because the spin lattices are canted. For the 0-h sample, the Morin transition is observed in the interval 185-209 K. After 2 h of ball milling the range is shifted toward 180-210 K and is less abrupt. After more than 4 h of milling time the transition becomes very broad, in agreement with the distribution in the crystallite sizes. The Morin temperature (given by the derivative in ZFC) is about 199 K at 0 h, 196 K at 2 h, and after 4 h the transition is already too broad to exhibit a clear maximum. In pure hematite, the Morin transition would be a step. Milling decreases the average crystallite size [23]; for low energy milling the grains are broken, the grain size decreases with a slight morphological change; for high energy milling, severe deformations occur, dislocations, lattice rotations, which lead to a reduction in crystallite size, that finally corresponds to an atomic level structural change. T_M, which depends on the size, decreases and is distributed over a broader temperature range: instead of a step the Morin transition becomes a slope [24].

The divergence between ZFC and FC is present for all samples and is extended over a large temperature interval for the samples milled at 4, 8 and 12 h, which indicates uncompensated magnetic moments. ZFC does not exhibit a sharp edge, so we do not witness classical superparamagnetism with a well-defined blocking temperature, T_B. The increase in the differences between ZFC-FC at 5 K with ball milling time indicates collective pinning rather than independent particles. The high effective anisotropy reflects collective pinning-disorder barriers, besides magneto-crystalline anisotropy, such that the grains are coupled, not independent. To summarize: the milling decreases the grains, induces stresses and defects, increases disorder, suppresses the Morin transition, broadens its temperature distribution, and stabilizes the canting (Dzyaloshinskii-Moriya antisymmetric exchange interactions), which explains the gradual increase in the magnetization with ball milling time.

CONCLUSION

Mixed oxide nanostructures of the type $xGa_2O_3*(1-x)a-Fe_2O_3$ with x=0.5 were successfully synthesized by high energy ball milling for times ranging from 0 to 12 hours. Magnetic measurements were performed by recording hysteresis loops in an applied magnetic field of 5 T at temperatures of 5 and 300 K and zero-field-cooling-field-cooling with a magnetic field of 200 Oe in the temperature interval 5-300 K. Magnetization and average coercive fields were studied as functions of ball milling time and temperature. The oxide system became considerably softer at long milling times and high temperatures. The Morin transition of hematite occurred over broad temperature ranges and was monitored as a function of ball milling time. The Dzyaloshinskii-Moriya antisymmetric exchange interaction explained the gradual increase in the magnetization with ball milling time.

ACKNOWLEDGMENT

This work was supported in part by the National Science Foundation, USA under grant DMR-0854794. Funding was also received from the Ministry of Research, Innovation and Digitization (Romania), CNCS/CCCDI-UEFISCDI core program under projects PC2-PN23080202 and 35PFE/2021.

Conflicts of Interests

There are no conflicts of interests regarding the work described in this paper.

References

[1]. Rozenberg, G., et al., High pressure structural studies of hematite Fe2O3. Physical Review B, 2002. 65: p. 064112.

[2]. Bergenmayer, W., et al., Ab Initio thermodynamics of oxide surfaces: O2 on Fe2O3 (0001). Physical Review B, 2004. 69: p. 195409.

[3]. Zheng, Y., et al., Quasicubic a-Fe2O3 nanopartcles with excellent catalytic performance. Journal of Physical Chemistry, 2006. 110: p. 3093-3097.

[4]. Wu, C., et al., Synthesis of hematite (a-Fe2O3) nanorods: Diameter-size and shape effects on their applications in magnetism, lithium ion battery, and gas sensors. Journal of Physical Chemistry, 2006. 110: p. 17806-17812.

[5]. Liu, J.Z., Morin transition in hematite doped with Iridium ions. Journal of Magnetism and Magnetic Materials, 1986. 54-57: p. 901-902.

[6]. Stroh, C., et al., Ruthenium oxide-hematite magnetic ceramic nanostructures. Ceramics International, 2015. 41: p. 14367-14375.

[7]. Chen, Y., et al., Bandgap engineering of gallium oxides by crystalline disorder. Materials Today Physics, 2021. 18: p. 100369.

[8]. Lorenzi, R., et al., Defect-assisted photocatalytic activity of glass-embedded gallium oxide nanocrystals. Journal of Colloid and Interface Science, 2022. 608: p. 2830-2838.

[9]. Chen, Y., et al., Electronic states of gallium oxide epitaxial thin films and related atomic arrangement. Applied Surface Science, 2022. 578: p. 151943.

[10]. Sudrajat H., et al., Gallium oxide nanoparticles prepared through solid state route for efficient photocatalytic overall water splitting. Optyk, 2020. 223: p. 165370.

[11]. Meligrana G., et al., Gallium oxide nanorods as novel, safe and durable anode materials for Li- and Na- ion batteries. Electrochimica Acta, 2017. 235: p. 143-149.

[12]. Su, T., et al., High-rate growth of gallium oxide films by plasma-enhanced thermal oxidation for solar-blind photodetectors. Applied Surface Science, 2023. 624: p. 157162.

[13]. Falkova, A.N., et al., Mechanoactivated interaction of hematite and gallium. Journal of Alloys and Compounds, 2009. 480: p. 31-34.

[14]. Pichorim, A., et al., Room temperature ferromagnetism in oxygen deficient gallium oxide films with cubic spinel structure. Materials Chemistry and Physics, 2022. 287: p. 126320.

[15]. Jubu, P.R., et al., Synthesis and characterization of gallium oxide in strong reducing growth ambient by chemical vapor deposition. Materials Science in Semiconductor Processing, 2021. 121: p. 105361.

[16]. Yang, Z., et al., Resistive random access memory based on gallium oxide thin films for powered pressure sensor systems. Ceramics International, 2020. 46: p. 21141-21148.

[17]. Glasser, S., et al., Effects of mechanochemical activation on the structural, magnetic and optical properties of yttrium iron garnet-graphene nanoparticles. Physica B, 2023. 650: p. 414501.

[18]. Sorescu, M., et al., Formation of skyrmion phase in the Fe-Co-Si system by mechanochemical activation. Physica B, 2024. 688: p. 416153.

[19]. Glasser, s., et al., Synthesis and characterization of gadolinium oxide-hematite magnetic ceramic nanostructures. Journal of Minerals and Materials Characterization and Engineering, 2023. 11: p. 1-15.

[20]. Sorescu, M., et al., Mechanochemical synthesis and Mössbauer characterization of neodymium oxide-hematite magnetic ceramic nanoparticles: Phase sequence and recoilless fraction. Materials Chemistry and Physics, 2022. 277: p. 125511.

[21]. Herzer, G., Effect of grain size on the coercivity of nanocrystalline ferromagnets. IEEE Transactions on Magnetics, 1990. 26: p. 1397-1402.

[22]. Chudnovsky, E.M., Random anisotropy in amorphous and nanocrystalline ferromagnets. Journal of Magnetism and Magnetic Materials, 1985. 54-47: p. 1097-1100.

[23]. Diamandescu, L. et al., Multifunctional GaFeO3 obtained via mechanochemical activation followed by calcination of equimolar nanosystem Ga2O3-Fe2O3. Nanomaterials, 2021. 11: p.57.

[24]. Diaz-Guerra, C., et al., Magnetic transitions in a-Fe2O3 nanowires. Journal of Applied Physics, 2009. 106: p. 104302.